# Evaluation of the Shrinking-Core Model for Examining the Kinetics of Film Formation in a Reactive Latex Blend

**Brian Boyars, Eric S. Daniels, Andrew Klein**

*Emulsion Polymers Institute and Department of Chemical Engineering, Lehigh University, 111 Research Drive, Bethlehem, Pennsylvania 18015*

Received 31 January 2005; accepted 11 April 2005
DOI 10.1002/app.22779
Published online in Wiley InterScience (www.interscience.wiley.com).

**ABSTRACT:** We prepared reactive latex blends from two copolymer latices comprised of *n*-butyl methacrylate (*n*-BMA) with acetoacetoxyethyl methacrylate and *n*-BMA/dimethylaminoethyl methacrylate to study the kinetics of film formation. We generated thin films by blending equal weights of the two latices. The films were then cured at temperatures ranging from 50 to 90°C. The extent of the crosslinking reaction was calculated from the crosslink density, which was determined from swelling measurements of the films in toluene. The shrinking-core model, a diffusion/reaction model, which was originally derived for combustion reactions of coal particles, was adopted to calculate the diffusion coefficient ($D_e$) and reaction rate constants from the extent of the reaction with time data. This model system exhibited a diffusion-controlled regime above 70°C and a reaction-controlled regime at temperatures below 70°C. In the reaction-controlled regime, the shrinking-core model predicted $D_e$ for the system, which was in agreement with literature values for *n*-BMA. In the diffusion-controlled regime, the model predicted a lower apparent value for $D_e$ but with an activation energy that was close to that obtained for *n*-BMA. The model was also used to examine the kinetics of the crosslinking reaction. The kinetic rate constants for the crosslinking reaction were also determined. The activation energy for the crosslinking reaction was 18.8 kcal/mol, which compared reasonably with the activation energy of 22.8 kcal/mol determined for the reaction between the functional monomers as small molecules.  J Appl Polym Sci 101: 3659–3665, 2006

**Key words:** coatings; core-shell polymers; crosslinking; modeling

## INTRODUCTION

The major uses for latices are in the coatings industry. The ease with which a strong film is produced is of great importance. Strength development in latex films depends on chain interdiffusion and entanglement, which for linear polymers, is very slow. The interpenetration depth scales with time to the one-quarter power and one radius of gyration is required for optimal film strength. Coalescing solvents are often used in industry to achieve faster diffusion. This is undesirable from an ecological viewpoint because coalescing solvents eventually leave the film and contribute to pollution. Reactive latex blends could potentially reduce the interpenetration distance required for strength development. This could result from the formation of crosslinks much earlier in the film-formation process compared to chain entanglements.

The major part of the experimental literature on reactive latices can be divided into three basic areas: the synthesis and characterization of latices containing functional groups,[1–3] the evaluation of the mechanical properties of films derived from these latices,[4–7] and the correlation of the mechanical properties with different formulation and process variables (e.g., type, amount, and location of the functional groups).[8–13]

A theoretical treatment of the reaction kinetics of a one-component reactive system with an added crosslinking agent was given by Aradian et al.[14,15] Their analysis defined a control parameter that relates the speed of the crosslinking reaction to the speed of polymer chain interdiffusion (i.e., a Damköhler number). Aradian et al.[14,15] defined two basic regimes of interest. When is greater than 1, the system is in the fast-reaction regime. In this regime, the crosslinking reaction dominates the film-formation process, and the resulting film tends to be sintered. When is less than 1, the system is in the slow-reaction regime. In this regime, the polymer chain interdiffusion dominates the film-formation process, which results in a more uniformly crosslinked film

Experimental work on the kinetics of film formation was discussed by Pham and Winnik[16] and Toshiyuki, Pinenq, and Winnik.[17] In the first system, the interdiffusion and reaction in a carbodiimide–carboxyl system was studied, and in the second, the influence of crosslinking in a single-component system with epoxy groups was investigated. Liu and Winnik[18] compared crosslinking and interdiffusion in an acrylic system with *N*-(isobutoxymethyl)acrylamide. In each system, chain interdiffusion and crosslinking were measured

*Correspondence to:* A. Klein (ak04@lehigh.edu).

separately. Chain interdiffusion was measured with nonradiative energy transfer, and crosslinking was measured through gel content. It was shown that interdiffusion was relatively fast at the beginning of the curing process and slowed significantly as the crosslinking reaction proceeded in all three cases. These approaches have illustrated the interconnection between crosslinking and interdiffusion in a reactive system, but they have not offered a model. The approach presented in this article is model-based and examines the two phenomena simultaneously.

## THEORY

The reactive latex system discussed in this article used crosslinking functionality in a two-component system by the copolymerization of acetoacetoxyethyl methacrylate (AAEM) or dimethylaminoethyl methacrylate (DMAEM) with *n*-butyl methacrylate (*n*-BMA) and the subsequent blending of the two latices together. The result was a latex consisting of two types of particles, one with incorporated acetoacetoxy functional groups and one with incorporated amino functional groups. This blend system was capable of interparticle crosslinking.

In a reactive latex, polymer chain interdiffusion and crosslinking both contribute to the morphology and mechanical properties of the derived film. For the crosslinking reaction to occur, the incorporated functional groups must diffuse through a polymer layer, come into contact with one another, and react. Analogous to this system is the shrinking-core model developed by Ishida and Wen[19] to model the gas–solid combustion of spherical coal particles. In coal combustion, oxygen molecules must diffuse through an inert ash layer that forms as the particles burn for the combustion to continue, whereas in a reactive latex, the incorporated functional groups must diffuse through the linear polymer or a crosslinked layer surrounding them for the crosslinking reaction to occur.

To use the shrinking-core model with a reactive latex blend, we made several assumptions. First, an effective and constant diffusion coefficient ($D_e$) was assumed because there are currently no known methods for calculating $D_e$ below the reptation time. The assumption of constant $D_e$ is perhaps valid for a system with a slow crosslinking reaction. If a system has a fast crosslinking reaction, the constant $D_e$ assumption may not hold because of the changing crosslink density ($\rho_c$) in the crosslinked layer. The second assumption was that every particle would be surrounded by particles containing the other functional groups and, thus, that all functional groups would play a role in the crosslinking reaction. Although this assumption was statistically inaccurate, the fraction of participating functional groups could be estimated from the plateau $\rho_c$ value. The third assumption was that the extent of the crosslinking reaction ($x$) could be followed by polymer swelling measurements. The last assumption was that the functional groups were uniformly distributed throughout the portion of the particle where the crosslinking reaction occurred. As is shown later, none of the assumptions we made limited the accuracy of the model.

Equation (1) was used to model reactive latices with the shrinking core model. In eq. (1), $t$ is time, and $K$ and $Y$ are fitted parameters. $x$ was calculated with eq. (2):

$$t(x,K,Y) = K[1 - (1 - x)^{\frac{1}{3}}]\left\{1 + \frac{Y}{6}[(1 - x)^{\frac{1}{3}} + 1 - 2(1 - x)^{\frac{2}{3}}]\right\} \quad (1)$$

$$x = \frac{M_c(\infty)}{M_c(t)} \quad (2)$$

where $M_c(t)$ is the molecular weight between crosslinks at time $t$ and $M_c(\infty)$ is the plateau molecular weight between crosslinks. We determined the parameters $K$ and $Y$ by fitting eq. (1) to the experimental data with a nonlinear least-squares estimation. Equations (3) and (4) relate $K$ and $Y$ to the reaction rate coefficient for the crosslinking reaction and $D_e$ for the system:

$$K = \frac{r_s}{k_r} \quad (3)$$

$$Y = \frac{r_s k_r}{D_e} \quad (4)$$

where $D_e$ is the effective diffusion coefficient, $r_s$ is the radius of the particle, and $k_r$ is the reaction rate constant.[20]

## EXPERIMENTAL

### Materials

We removed monomethylether hydroquinone inhibitor from *n*-BMA (Sigma-Aldrich) and DMAEM (Sigma-Aldrich) by passing the monomers through an inhibitor removal column (Sigma-Aldrich) before use. AAEM (Eastman Chemical), Igepal CO-880 [$(C_2H_4O)_nC_{15}H_{24}O$; n = 20–30; Rhodia], potassium persulfate (KPS; Sigma-Aldrich), V-50 [2,2′-azobis(2-methylpropionamidine) dihydrochloride; Wako], ethyl benzene (Sigma-Aldrich), toluene (VWR Scientific), standardized sodium hydroxide solution (JT Baker), standardized hydrochloric acid solution (JT Baker), and dioxane (Sigma-Aldrich) were used without further purification. We deionized the water and purged it of oxygen by bubbling nitrogen through it before use.

**TABLE I**
**Summary of Batch Polymerization Recipes**

| Component | Amount (g) |
|---|---|
| *n*-BMA | 70.00 |
| AAEM or DMAEM | 5.00 |
| Deionized $H_2O$ | 175.00 |
| Igepal CO-80 | 7.93 |
| KPS | 0.70 |

### Latex synthesis

*n*-BMA latices containing acetoacetoxy or amino functional groups were prepared by batch or semicontinuous emulsion polymerization processes. Tables I and II show the recipes used for the latex syntheses. All of the reactions were carried out in a four-necked, 500-mL reaction flask immersed in a water bath at 60°C. The flask was equipped with a Teflon stirring paddle and a Friedrichs condenser. The stirring rate was approximately 200 rpm. The flask was also continuously purged with nitrogen to prevent oxygen from inhibiting the polymerization. For batch polymerizations, all of the components were charged to the flask and held at 60°C for 24 h. For semicontinuous polymerizations, the seed stage reactants were charged to the flask and held at 60°C for 30 min. The feed stage *n*-BMA and functional monomer were thoroughly mixed and fed with a Teflon feed line and a Harvard apparatus (model 22M) syringe pump over the course of 6 h. The feed-stage initiator solution was fed in parallel with the monomer with a separate feed line and Harvard apparatus (model 22M) syringe pump over the course of 6 h. All of the reactions had an 18-h postfeed time to ensure complete conversion.

### Solid content and conversion

Gravimetric analysis was used to determine the solid content and conversion of the latices. Samples (2.5 mL) were removed from the reactor, quenched in ice to stop the polymerization, weighed, inhibited with several drops of 1% aqueous hydroquinone solution to prevent further polymerization, and then dried to a constant weight at 70°C.

### Particle size characterization

Dynamic light scattering (Nicomp, model C370) was used to determine the particle size of the latices.

### Thermal transitions

Differential scanning calorimetry (TA Instruments, model 2920) was used to determine the glass-transition temperature ($T_g$) of the latices. Samples were dried at room temperature and heated from 10 to 80°C at a rate of 10°C/min.

### Swelling measurements

Samples of both functional latices containing the same amount of polymer were mixed and diluted to 7% solids and cleaned with a serum replacement cell with 50-nm filter membranes.[21] We prepared the films by drying the cleaned latex on a glass plate covered with DuPont Tedlar film for up to 45 days at temperatures ranging from 50 to 90°C. The evolution of the molecular weight between crosslinks ($M_c$) and $\rho_c$ as a function of the cure time were determined. Pieces of the crosslinked films were cut and weighed, placed in a preweighed, wide-mouthed bottle, and immersed in toluene at approximately 100 times the weight of the film. The bottles were then sealed and slowly rotated end-over-end at 30 rpm for 48 h. The swollen film was then removed, blotted dry, and quickly weighed. The sample was then allowed to dry to constant weight in a fume hood. $M_c$ and $\rho_c$ were calculated with eqs. (5)–(9):[22]

$$\chi_1 = \frac{V_1(\delta_s - \delta_p)^2}{RT} \tag{5}$$

$$V_s = \frac{W_o}{\rho_p} + \frac{W_s - W_o}{\rho_s} \tag{6}$$

$$c = \frac{W_o}{\rho_p V_s} \tag{7}$$

$$M_c = \frac{-V_1\rho_p(c^{1/3} - c/2)}{ln(1 - c) + c + \chi_1 c^2} \tag{8}$$

$$\rho_c = \frac{\rho_p}{M_c} \tag{9}$$

where $\chi_1$ is the Flory Chi parameter; $V_1$ ($cm^3/mol$) is the molar volume of the solvent; $\rho_p$ ($g/cm^3$) and $\rho_s$ ($g/cm^3$) are the densities of the polymer and solvent, respectively; $\delta_p$ $(J/cm^3)^{1/2}$ and $\delta_s$ $(J/cm^3)^{1/2}$ are the solubility parameters of the polymer and solvent, respectively; $W_o$ (g) and $W_s$ (g) are the weights of the unswollen and swollen films, respectively; $V_s$ ($cm^3$) is

**TABLE II**
**Summary of Semicontinuous Polymerization Recipes**

| | Amount | |
|---|---|---|
| | Seed stage | Feed stage |
| n-BMA (g) | 7.0 | 63.0 |
| AAEM or DMAEM (g) | 0.0 | 5.0 |
| Deionized water (g) | 150.0 | 0.0 |
| Igepal CO-880 (g) | 7.93 | 0.00 |
| V-50 solution (mL)[a] | 5 | 20 |
| Time (h) | 0.5 h | 6.0 h |

[a] Prepared by the dissolution of 1.0 g of V-50 in 20 mL of deionized $H_2O$ and dilution to 25 mL.

**TABLE III**
**Results of Latex Characterization**

| Latex | Batch functional AAEM | Semicontinuous functional AAEM | Batch functional DMAEM | Semicontinuous functional DMAEM |
|---|---|---|---|---|
| $D_n$ (nm) | 73 | 70 | 69 | 49 |
| $D_v$ (nm) | 73 | 76 | 70 | 65 |
| $M_n$ (g/mol) | 122,000 | 67,000 | 50,000 | 97,000 |
| $M_w$ (g/mol) | 628,000 | 272,000 | 181,000 | 393,000 |
| $T_g$ (°C) | 35.0 | 38.0 | 36.7 | 32.4 |

$D_n$ = number-average particle diameter; $D_v$ = volume-average particle diameter; $M_n$ = number-average molecular weight; $M_w$ = weight-average molecular weight.

the volume of solvent in the swollen film; $c$ is the concentration of the solvent in the polymer; $M_c$ (g/mol) is the molecular weight between crosslinks; and $\rho_c$ (mol/cm$^3$) is the crosslink density. The values for $\delta_p$ and $\rho_p$ were assumed to be the same as *n*-BMA because no literature values were available for the copolymers.

### Molecular weight determination

Gel permeation chromatography (with a Waters 515 HPLC pump and a Waters 410 differential refractometer) was used to determine the molecular weights of the latices. Samples of the blended latex were dried at room temperature and dissolved in tetrahydrofuran.

### Reaction kinetics of the functional monomers

Gas chromatography (Hewlett-Packard, model 5890A, with an HP-5 Ph Me Silicone column and split injection port with a 8.8:1 split ratio) was used to study the kinetics of the functional monomer reaction. Equal amounts of the two functional monomers were mixed and reacted at temperatures from 50 to 90°C. Samples were taken every hour and dissolved in toluene with ethyl benzene as an internal standard. Samples were injected into the gas chromatograph and vaporized at 150°C. The column oven was held at 80°C for 2 min, ramped to 100°C at 20°C/min, held at 100°C for 5 min, ramped to 150°C at 20°C/min, and held at 150°C for 10 min. Components were detected with a flame ionization detector at 300°C.

### Determination of the surface functional group concentration

Conductometric titrations were carried out to determine the location of the functional groups within the polymer particles. The individual latices were diluted to about 10% solids and cleaned with a serum replacement with 50-nm membranes to remove any water-soluble polymer. A small sample of the latex was then placed in a wide-mouthed jar and diluted with deionized water. A small amount of dioxane was then added, and the entire jar was blanketed with argon. For the amino-functional latices, excess hydrochloric acid was then added and allowed to equilibrate with the amino groups. The excess acid and protonated amino groups were then backtitrated with sodium hydroxide. For the acetoacetoxy-functional latices, excess sodium hydroxide was added and allowed to equilibrate with the acetoacetoxy groups. The excess base and deprotonated acetoacetoxy groups were then backtitrated with hydrochloric acid. The serum from the uncleaned latices was separated by ultracentrifugation at 30,000 rpm for 2 h at 20°C, and the serum was titrated in the same manner to determine if any functional groups were present as water-soluble polymer.

## RESULTS AND DISCUSSION

Table III shows the results of the characterization of the individual latices before blending. Each pair of functional latices had similar $T_g$'s and relatively broad molecular weight distributions. In both sets of batch polymerizations, the particle size distribution was relatively narrow. The semicontinuous polymerizations showed a slight broadening of the particle size distributions, which indicated that there was some secondary nucleation during the feed-stage polymerization. In addition, the amino-functional latices produced slightly smaller particles than the acetoacetoxy-functional latices.

Figure 1 shows the evolution of $\rho_c$ as a function of time at different temperatures for the films cast from the batch latex blends. Each curve showed a sharp increase in $\rho_c$ that eventually reached a plateau. These results were consistent with other crosslinking studies.[14–16] We analyzed $\rho_c$ with the shrinking-core model for each temperature to determine the apparent $D_e$ for the system and $k_r$ for the crosslinking reaction. Figure 2 shows a representative curve fit of the shrinking-core model [eq. (1)] to the experimental data at 50°C. Boczar et al.[23] showed an Arrhenius relationship for the *n*-BMA diffusion data from nonradiative energy transfer measurements. Figure 3 shows a plot of the $D_e$ values estimated with the shrinking-core model compared to those values determined by Boczar et al.[23]

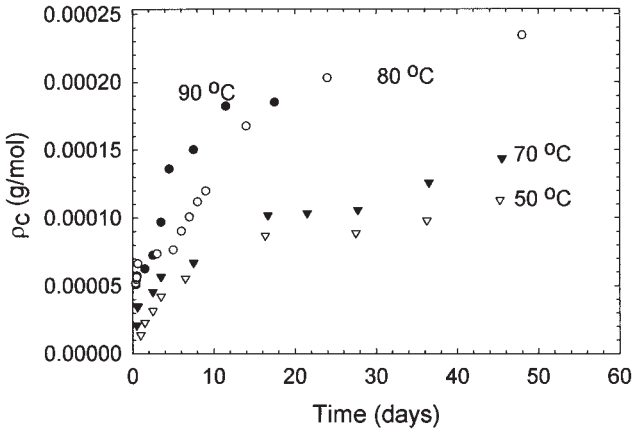


**Figure 1** Comparison of the evolution of $\rho_c$ in films cast from latices prepared with a batch process at different temperatures.

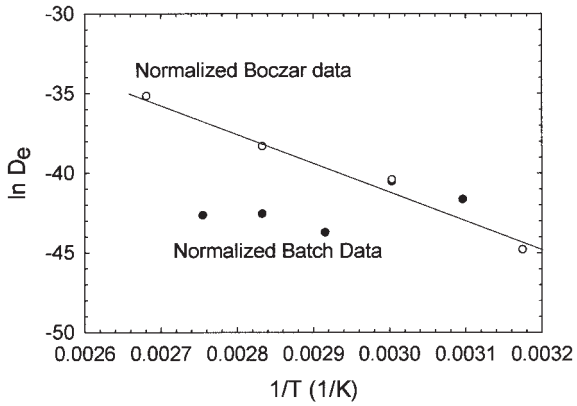


**Figure 3** Comparison of $D_e$ as determined by the shrinking-core model with data published by Boczar et al.[23] with the molecular weight normalized to 125,000 g/mol.

normalized to the same molecular weight ($D_e \propto M_w^{-2}$, $M_{\text{Boczar}}$ = 145,000 g/mol, $M_{\text{Norm}}$ = 125,000 g/mol, where $M_w$ is the weight-average molecular weight).[24]

At temperatures above 70°C, the model showed a deviation from the values published by Boczar et al.[23] This decrease in $D_e$ most likely arose from the faster crosslinking reaction compared to diffusion and generated a crosslinked shell layer. At the lower temperatures (<70°C), the film formation was likely to be reaction-controlled (i.e., the rate of diffusion was faster than the rate of reaction), and most of the diffusion took place through a linear network. As a result, the shrinking-core model correctly predicted the value of $D_e$ at low temperatures. At higher temperatures, the system may have become diffusion-controlled, and most of the diffusion took place through a crosslinked network. Consequently, the shrinking-core model predicted a value for $D_e$ lower than those in the literature. However, the slopes obtained from the reaction and diffusion-controlled regions were the same within experimental uncertainty as the slope from the data published by Boczar et al.[23]

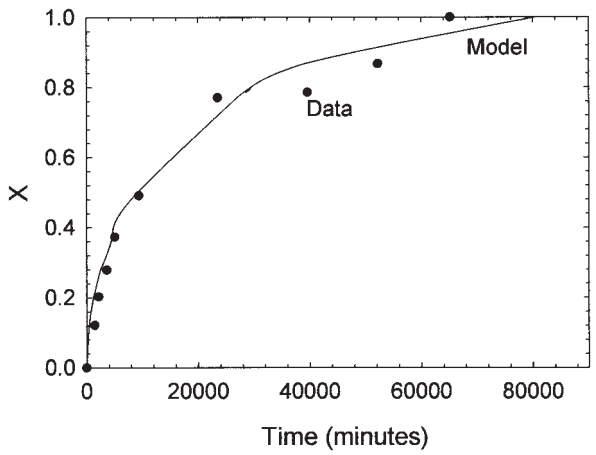


**Figure 2** Sample curve fit of the shrinking-core model to the experimental data at 50°C.

Evidence to support the existence of the reaction- and diffusion-controlled regimes was found through the examination of the concentration of functional groups at the surface of the polymer particles. For the amino-functional latices made with a batch emulsion polymerization process, the conductometric titration detected 90.0 ± 2.5% of the functional groups at the particle surface. For the amino-functional latices made with a semicontinuous polymerization process, only 17.9 ± 2.1% of the functional groups were detected by the titration. In the case of the acetoacetoxy-functional latices made with a batch polymerization process, 39.7 ± 5.1% of the functional groups were detected with the titration process. For the acetoacetoxy-functional latices made with a semicontinuous polymerization process, the titration detected 29.0 ± 2.5% of the functional groups. The serum titration did not indicate any functional groups present as water-soluble polymer in any of the latices, which implied that the balance of the functional groups were buried inside the particles.

For the higher curing temperatures where the system was in the diffusion-controlled regime, the majority of the crosslinking reaction took place near the surface of the particles due to the faster crosslinking reaction. Therefore, films cast from latices prepared with a batch polymerization process should have had higher $\rho_c$ values due to the higher concentration of functional groups near the particle surface. Figure 4 compares the evolution of $\rho_c$ in films cast from latices prepared with batch or semicontinuous polymerization processes at high temperatures. At lower curing temperatures where the system was reaction-controlled, the crosslinking reaction was not concentrated near the surface of the particles because the crosslinking reaction was slower. Therefore, the films cast from latices made with semicontinuous polymerization processes had higher $\rho_c$ values because crosslinking could occur continuously throughout the particles

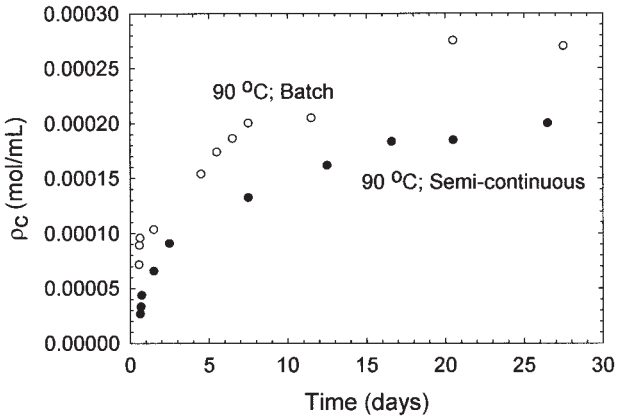


**Figure 4** Comparison of $\rho_c$ between films cast from latices made with a batch or semibatch polymerization process at 90°C.

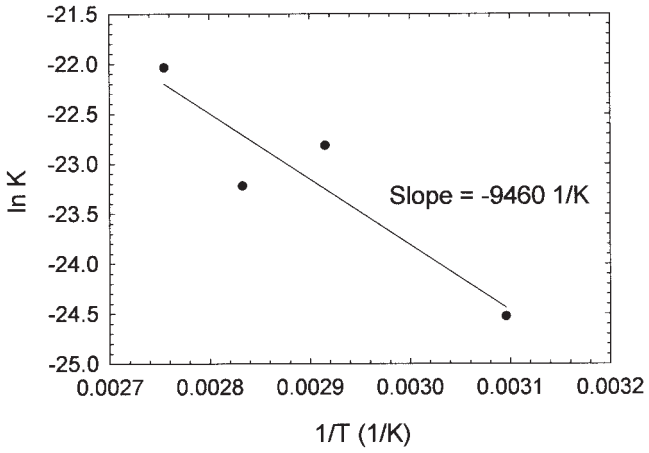


**Figure 6** Correlation of $K$ with temperature.

(whereas it could only occur at the particle surface in batch latices).

Figure 5 compares the evolution of $\rho_c$ in films cast from latices prepared with batch or semicontinuous polymerization processes at lower temperatures.

To further validate the usefulness of the shrinking-core model, the kinetic rate constants from the model were compared to the experimental data. The reaction rate ($r$) data is presented in an Arrhenius plot in Figure 6. No literature values were found for comparison. Therefore, a kinetic study of the crosslinking reaction with the functional monomers as small molecules was carried out. $r$ for the small-molecule crosslinking reaction is given by eq. (10):

$$r = k[\mathrm{AAEM}]^m[\mathrm{DMAEM}]^n \qquad (10)$$

where $k$ is the rate constant; [AAEM] and [DMAEM] are the concentrations of the acetoacetoxy and amino monomers, respectively; and $m$ and $n$ are the orders of the reaction with respect to each reactant.[25] If the reaction was assumed to be elementary and the initial reactant concentrations were the same, the initial $r$ was proportional to the rate constant, and therefore, a plot of ln(Initial rate) versus $1/T$ would be linear, with the slope proportional to the activation energy. Figure 7 shows a typical plot of the moles of DMAEM versus time for the small-molecule crosslinking reaction at 60°C. The slope of Figure 7 is the initial $r$. Figure 8 shows a plot of ln(Initial rate) versus $1/T$ for the gas chromatography experiments. The activation energy calculated from the slope of the line was 22.8 kcal/mol compared with 18.8 kcal/mol as determined with the shrinking-core model.

## CONCLUSIONS

The kinetics of film formation of a model two-component reactive latex were analyzed with the shrinking-core model. Nonlinear least-squares estimation applied to the crosslinking data allowed the effective $D_e$ and $k_r$ values to be calculated. Several assumptions

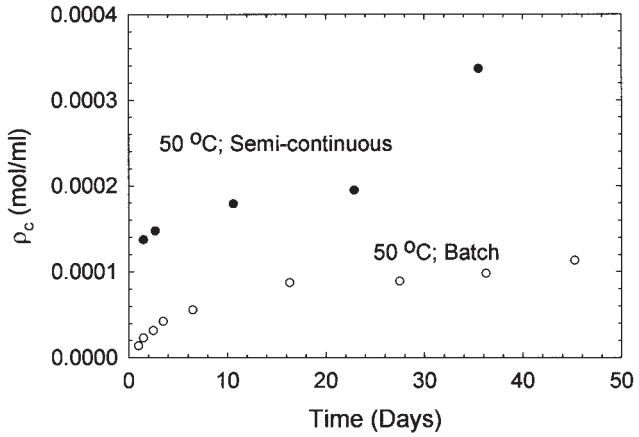


**Figure 5** Comparison of $\rho_c$ between films cast from latices made with a batch or semibatch polymerization process at 50°C.

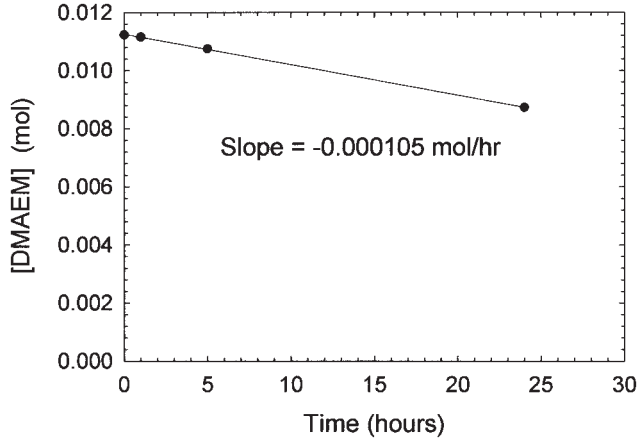


**Figure 7** Plot of [DMAEM] versus time at 60°C.

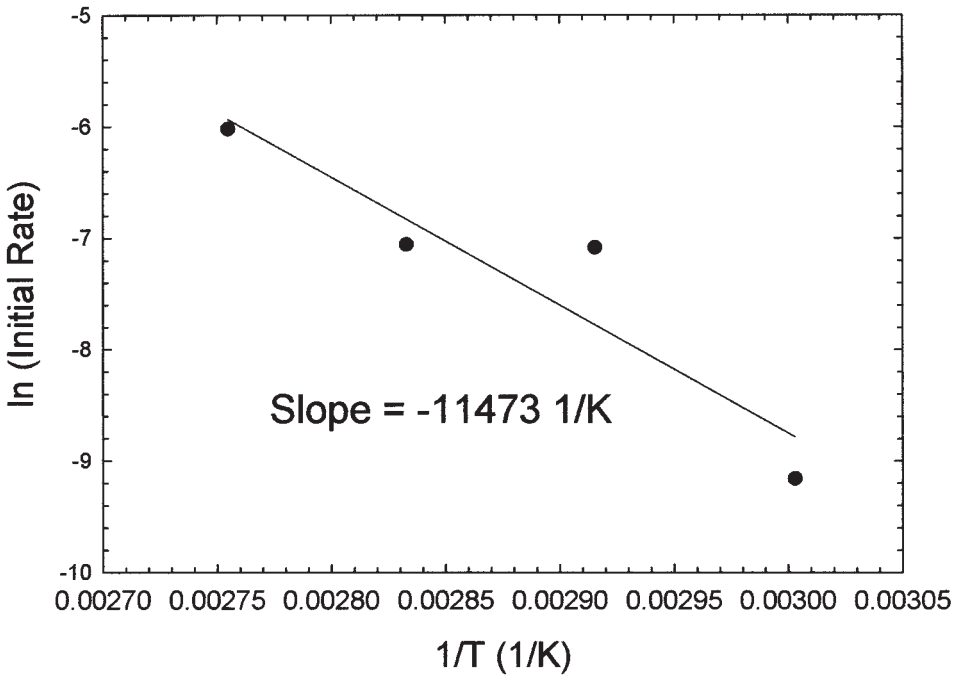


**Figure 8** Plot of ln(Initial rate) versus $1/T$.

were made to apply the model to this system; however, none of the assumptions were crippling.

The analysis based on the model system showed a reaction-controlled regime at temperatures below 70°C and a diffusion-controlled regime above 70°C. In the reaction-controlled regime, the model accurately predicted the value of $D_e$. In the diffusion-controlled regime, the model predicted an apparent value for $D_e$ that was lower than the reaction-controlled regime. The effective $D_e$ values estimated by the model yielded an apparent activation energy of diffusion that was in agreement with values found in the literature.

The shrinking-core model was also used to determine the crosslinking $k_r$ and activation energy. The activation energy agreed with values obtained by kinetic studies of the same reaction with the functional monomers acting as small molecules.

## References


1. Collins, M. J.; Taylor, J. W. U.S. Pat. 5,998,543 (1999).
2. Collins, M. J.; Taylor, J. W.; Murray, D. L. U.S. Pat. 6,060,556 (2000).
3. Stockl, R. R.; Collins, M. J.; Taylor, J. W. U.S. Pat. 6,417,267 (2002).
4. Zhao, Y.; Urban, M. W. Macromolecules 2000, 33, 8426.
5. Park, Y. J.; Kim, J. H. Colloid Surf A 1999, 153, 583.
6. Park, Y. J.; Kim, J. H. J Ind Eng Chem 1997, 3, 298.
7. Park, Y. J.; Kim, J. H. Polym Sci Eng 1998, 38, 884.
8. Park, Y. J.; Monteiro, M. J.; van Es, S.; German, A. L. Eur Polym J 2001, 37, 965.
9. Feng, J.; Pham, H.; Macdonald, P.; Winnik, M. A.; Geurts, J. M.; Zirkzee, H.; van Es, S.; German, A. L. J Coat Technol 1998, 70, 57.
10. Geurts, J. M. Ph.D. dissertation, Eindhoven University, Eindhoven, The Netherlands, 1997.
11. Xu, J.; Dimonie, V. L.; Sudol, E. D.; El-Aasser, M. S. J Appl Polym Sci 1998, 69, 965.
12. Xu, J.; Dimonie, V. L.; Sudol, E. D.; Shaffer, O. L.; El-Aasser, M. S. J Appl Polym Sci 1998, 69, 977.
13. Xu, J.; Dimonie, V. L.; Sudol, E. D.; Klein, A.; El-Aasser, M. S. J Appl Polym Sci 1998, 69, 985.
14. Aradian, A.; Raphaël, E.; de Gennes, P.-G. Macromolecules 2000, 33, 9444.
15. Aradian, A.; Raphaël, E.; de Gennes, P.-G. Macromolecules 2002, 35, 4036.
16. Pham, H. H.; Winnik, M. A. Macromolecules 1999, 32, 7692.
17. Toshiyuki, T.; Pinenq, P.; Winnik, M. A. Macromolecules 1999, 32, 6102.
18. Liu, R.; Winnik, M. A. Macromolecules 2001, 34, 7306.
19. Ishida, M.; Wen, C. Y. AIChE J 1968, 14, 311.
20. Smith, J. M. Chemical Engineering Kinetics, 2nd ed.; McGraw-Hill: New York, 1970; p 580.
21. Ahmed, S. M.; El-Aasser, M. S.; Pauli, G. H.; Poehlein, G. W.; Vanderhoff, J. W. J Colloid Interface Sci 1980, 73, 388.
22. Rodriguez, F. Principles of Polymer Systems, 2nd ed.; McGraw-Hill: New York, 1982; p 26
23. Boczar, E. M.; Dionne, B. C.; Fu, Z.; Kirk, A. B.; Lesko, P. M.; Koller, A. D. Macromolecules 1993, 26, 5778.
24. Wool, R. P. Polymer Interfaces: Structure and Strength; Hanser: Cincinnati, OH, 1995; p 167.
25. Froment, G. F.; Bischoff, K. B. Chemical Reactor Analysis and Design, 2nd ed.; Wiley: New York, 1990; p 6.